Pageoph, Vol. 115 (1977), Birkhäuser Verlag, Basel

Anomalous Seismicity prior to Rock Bursts: Implications for Earthquake Prediction

By B. T. BRADY[1])

Abstract – Anomalous seismicity changes (increase followed by a decrease) were recorded prior to three moderate rock bursts in the Star mine, Burke, Idaho. In each case, based upon the anomalous seismicity behavior, miners were evacuated or were prohibited from entering active mine stopes that were located in the immediate vicinity of the seismicity buildup prior to the bursts. Analyses of pre- and post-seismic activity are interpreted in terms of, and shown to be consistent with, the inclusion theory of failure. Implications of these observational results for the problem of rock bursts and earthquake prediction are discussed.

Key words: Seismicity; Earthquake prediction; Stress *in-situ*.

Introduction

Evidence is presented here that seismic precursor effects, such as anomalous seismicity behavior, were observed prior to rock bursts that occurred in a deep ($\sim$2.3 km) silver mine in northern Idaho. This behavior appears to be similar to that reported to precede some earthquakes and consists of a dramatic increase of seismicity in the hypocentral region of the impending burst, followed by a distinct decrease prior to the occurrence of the burst [1, 3, 5]. Seismicity anomaly information for these rock bursts and their implications for earthquake prediction are discussed.

Rock bursts at the Star mine

The Star mine, Burke, Idaho, is the deepest lead–zinc mine in the world and is located in the Coeur d'Alene mining district of northern Idaho. The Star mine occupies the westerly portion of the Star–Morning ore body, and both the Star and Morning mines are presently operated by the Hecla Mining Co. as the Star Unit.

The Star–Morning ore shoot is in a nearly vertical shear zone striking N 79° W (Fig. 2) and has a maximum strike length of approximately 1.3 km and an average stoping width of 3 meters. Wall rock is almost entirely dry, brittle, Precambrian Revett Quartzite. The principal mining method is horizontal-slice cut-and-fill stoping. In the lower levels of this mine, where the walls are subject to high stress, the ore body is developed by lateral drifts of 60 meters' average vertical separation in one

[1]) Physicist, U.S. Department of the Interior, BuMines, Denver Mining Research Center, Denver, USA.

of the walls with crosscuts through the ore. A blind stoping method is used with cribbed raises carried upward from the crosscuts in the ore zone (for details on the mining method and terminology, refer to [6]).

Detailed microseismic monitoring of potential rock burst zones in the Star mine was begun in 1975. The Star system consists of 21 geophones and associated peripheral computer equipment (see [7] for system details). The geophones are located on levels 6900, 7100, 7300, 7500, and 7700 (numbers refer to distances in feet measured from the surface entrance to the Star mine, 1 foot = 0.308 meter). The Star microseismic system covers approximately 490 meters and 215 meters parallel and normal, respectively, to the strike of the ore body. The minimum distance between any two geophones in the Star mine in approximately 50 meters. Complete details as to geophone locations within the Star mine are available elsewhere [7, Fig. 3].

Once a seismic event occurs and is picked up by a geophone, the signal is amplified at the geophone location, filtered, and transmitted to a voltage monitor. If the signal exceeds a preset threshold level of 0.5 volt peak-to-peak, a 15-volt pulse is transmitted by the voltage monitor to the computer and the event is registered. At this time, a 100 ms (1 ms = 1 millisecond) time window is opened. If four additional geophones are triggered by the event, the event is registered and located.

The average V_p velocity between geophones is determined by detonating one stick of 60% dynamite in known locations and observing the travel time to various geophones. Experimental results suggest an average velocity of 5.5 km/sec [7]. These explosions are consistently located to within 6 meters of the known source. Thus, location accuracy of seismic events that occur within the Star system is probably within a spherical region of radius less than 10 meters surrounding the source.

Unfortunately, information relating to magnitudes and fault plane solutions for the seismic events reported in this article is not available. However, surface seismographs located within the Coeur d'Alene mining district do permit a relative determination of the relative strength of the seismic event. For example, a typical rock burst will be recorded on the surface seismographs, while the individual seismic events that *precede* and *follow* (aftershocks in this article) the burst are generally too low in strength to be registered.

The seismicity behaviors of three rock bursts are examined in detail in this article. For sake of brevity, I have combined both the observational data of each burst and its interpretation in terms of the inclusion theory of failure in the analysis of the burst. The distinction between observation and interpretation is made clear throughout the text. In addition, it may be useful for the reader to be aware that the seismicity, as indicated by the number of events per day, in the Star mine shows that seismicity prior to rock bursts exhibits a *clear* increase (approximately 10 events per day [7, Fig. 9]) over a normal background level of approximately 8 events per day. For example, in the two months that preceded the rock bursts discussed in this article, the average number of events that occurred in a quarter day period (6 hours) was approximately two (2) with a standard deviation of ($\pm$) two (2). The 'background'

seismic events occurred over a broad region (usually a region whose dimensions are at least a factor of five (5) over an average dimension of the aftershock region produced by the rock burst). In addition, there is no tendency for these 'background' events to cluster spacially. The increase in seismicity prior to rock bursts reported in this article exhibit both a spacial as well as a temporal clustering that are statistically significant.

The 3 September 1975 rock burst

A moderate burst ($M_L < 1.5$) occurred on the 7500 level of the Star mine at 10:09:04 a.m. (18:09:04, UTC) on 3 September 1975. The burst was preceded by a dramatic increase of seismic activity in a localized region, which was followed by a distinct decrease prior to the burst as shown in Fig. 1. *Miners were evacuated from the stope (located in the immediate area of this seismic buildup) at this time.* In Fig. 1,

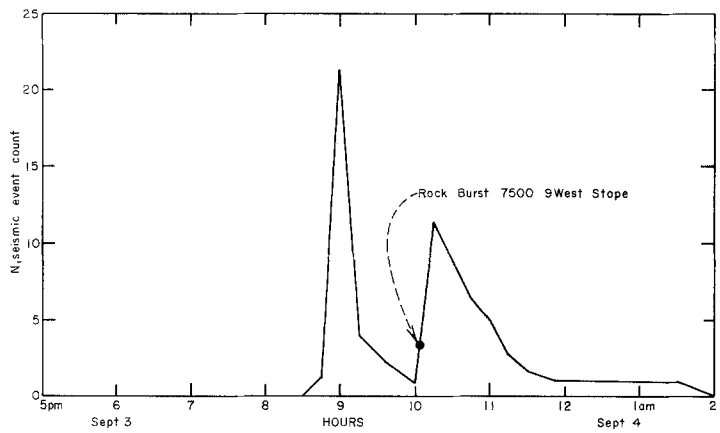

Figure 1
Seismic count (N) against time (hours) for 3 September rock burst. Seismic event count, N, refers to events that form the inferred primary inclusion zone of the impending burst.

number of seismic events refers to the number of events within a 15 minute time window. Table 1 lists seismic event numbers and their time of occurrence prior to the burst. Figures 2 and 3 illustrates the locations of the seismic events projected onto the horizontal plane (Fig. 2) and the projections of the aftershocks and their relationship to the mainshock onto the vertical plane along sections A–A' (Fig. 3a) and B–B' (Fig. 3b).

Four results are noteworthy from these data. *First*, the rapid increase of seismic activity prior to the burst was primarily associated with events 1 through 14 (Table 1, circles in Fig. 2), outlining a zone of early intensified activity (the shaded, circular zone shown in Fig. 2). The relative area, A_i, of this zone that apparently contains and is delineated by these events (marked by an asterisk in Table 1, circles in Fig. 2) is

approximately 7.86×10^5 cm^2, and the total time, τ_d, required for the formation of this circularly shaped region was 188 seconds. *Second*, the seismic events that followed (squares, Figs. 2 and 3) the formation of this zone were concentrated outside this circular zone and were primarily located near the outer boundaries of what was to be

Table 1
Seismic event number and time prior to 3 September burst

Event number	Time (a.m.)	Event number	Time (a.m.)
1*	9:00:32	15	9:05:53
2	9:00:38	16	9:06:09
3*	9:00:48	17	9:08:46
4*	9:00:53	18	9:10:44
5	9:00:55	19	9:22:27
6*	9:00:57	20	9:24:32
7	9:01:11	21	9:30:40
8*	9:01:38	22	9:44:52
9*	9:01:39	23	10:01:03
10	9:02:29	24	10:01:58
11	9:02:32	25	10:02:08
12*	9:02:40	26	10:02:24
13*	9:03:00	27	10:02:42
14*	9:03:38	28	10:05:10

Burst was event number 29 and occurred at 10:09:04 a.m.
* Events that are taken to have formed the primary inclusion zone.

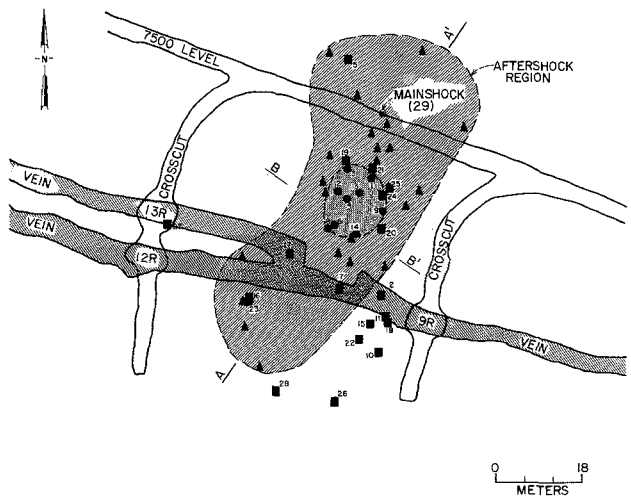

Figure 2
Plan view of 7500 level of the Star Mine including aftershock region, 'primary inclusion zone', and burst epicenter of 3 September 1975, rock burst. Circles refer to events that form the inferred primary inclusion zone of the impending burst; squares to pre-burst events not involved in the formation of the primary inclusion zone; triangles to events following the burst.

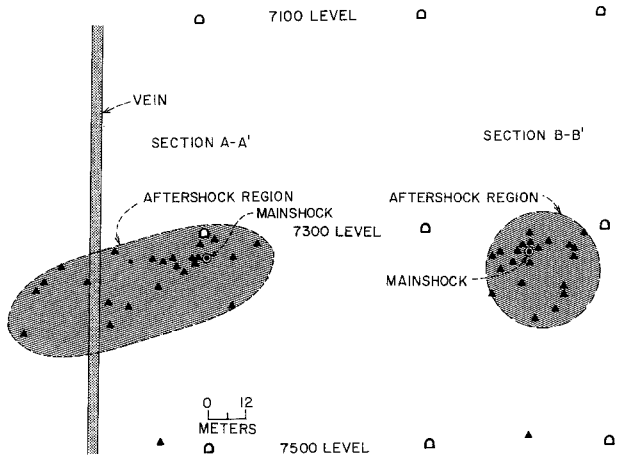

Figure 3
Vertical section of aftershock region of 3 September 1975, rock burst sections *A–A'* (a) and *B–B'* (c). Symbols (circles, squares, triangles) have the same meaning as in Fig. 2.

the aftershock region, or just outside the initially formed, circular zone (events 19–21, 24, and 25). Of particular interest, note that the events that followed the formation the primary inclusion zone were concentrated in a direction that was the eventual rupture propagation direction. Activity then abruptly diminished after event 25 for about 6.5 minutes until the burst occurred at 10:09:04 a.m. (18:09:04, UTC), and was followed by 22 aftershocks (triangles, Figs. 1a, b, and c) that defined an elliptical zone of area, A, equal to approximately 1.74×10^7 cm^2. The total time to the burst, measured from the initiation of seismic activity *assumed* to signal the growth (event 1, Table 1) of the primary inclusion zone, was 68.5 minutes. *Third*, the cross sections of the aftershock zone reveal an ellipsoidal zone (Figs. 3a and 3b) whose major axis is parallel to the eventual rupture propagation direction. In particular, note the circularly shaped cross section of this ellipsoid (Fig. 3b). This geometry is remarkably similar to that of the aftershock zone generally predicted by the inclusion theory when the far-field least and intermediate principal stresses are equal, an observation consistent with *in situ* stress measurements in this mine (Table 2) ([3, 4], see reference [4] Fig. 1). This figure suggest a 'volumetric' failure mechanism of this burst. However, the location accuracy of these events (± 10 meters) signifies that a 'planar' (fault) failure mechanism cannot be ruled out.

Table 2
In situ *stress distribution at east lateral drift 7300 level – Star mine*

Stress	Magnitude (kb)	Bearing
Major horizontal (σ_1)	0.66	N 14° W
Minor horizontal (σ_3)	0.42	N 76° E
Vertical (σ_2)	0.43	—

Fourth, the burst hypocenter was located approximately 8 meters from the predicted (on the basis of the inclusion theory of failure [3]) location on the boundary of the primary inclusion zone. This apparent displacement may or may not be real, as it falls within the reliability of the location accuracy of the microseismic system. However, this displacement is consistent with the framework of the inclusion theory in that, as the focal volume of the impending burst is predicted to become elastically stiffer than its immediate surroundings, the seismic velocities will increase [3]. This predicted increase would result in a migration of the actual burst hypocenter away from the boundary of the primary inclusion zone, as is shown in Fig. 2. To account for a relative displacement of this magnitude ($\simeq 8$ meters) of the burst hypocenter, a v_p increase of approximately 8% would be required in the area that was to become the aftershock region.

Theoretical and experimental studies have shown that the predicted functional relationships of the time required to form the primary inclusion zone (τ_{do}) and the time required for the failure to occur (τ_0) to the areas A_i and A are [3]:

$$\begin{aligned} \tau_{do} &= 2.43 \times 10^{-4} A_i \\ \tau_0 &= 2.43 \times 10^{-4} A, \end{aligned} \tag{1}$$

where times and areas are measured in seconds and square centimeters, respectively. Studies by the United States Bureau of Mines in the Galena mine, Wallace, Idaho, have also shown that a lower limit to the ratio τ_0/τ_{do} is 12.5 in hard, brittle rock [3]. Thus, once τ_d is known, a minimum predicted time to the burst is possible. Based upon the above observational data, the minimum predicted time to the 3 September burst is 40 minutes, where the observed values of τ_d (= 188 s) is used for τ_{do}. This value compares quite favorably with the observed value of 68.5 minutes. However, based upon the observed areas, A_i and A, the 'predicted' times for τ_{do} and τ_0 from equation (1) are 191 seconds and 70.3 minutes, respectively, in excellent agreement with observation. Thus, based on the observed seismicity increase that occurred within a highly localized region followed by a decrease, this burst was theoretically predictable, and the analysis further admits a more realistic estimate of the ratio τ/τ_d ($= \tau/\tau_{do} = 21.8$) required for accurate prediction time of future failures in this mine, assuming that the failures occur under comparable conditions.

This rock burst was *not* detected by the Newport, Wash., seismic station, operated by the United States Geological Survey. The Newport station, which is located approximately 150 km from the Star mine, is capable of detecting events of magnitude greater than $M1.5$ in the Coeur d'Alene district (KERRY, USGS, personal communication 1976). The functional relationship between aftershock area, A, and magnitude, M, can be estimated by using the Utsu relationship, $\log_{10} A = M + 6.3$, where A is in square centimeters [3]. Substituting the observed area of 1.74×10^7 cm^2 into this equation gives an estimated magnitude of $M0.9$ for the 3 September burst, well below the threshold value of $M1.5$.

The 24 October 1975 rock burst

A rock burst whose strength was considerably larger than the 3 September burst, but not detected at the Newport, Wash., seismic station, occurred in nearly the same location as the latter event. The burst was also preceded by a dramatic increase in seismic activity, which was followed by a distinct decrease prior to the burst, as shown in Fig. 4. *Miners were evacuated from the stope region at this time.*

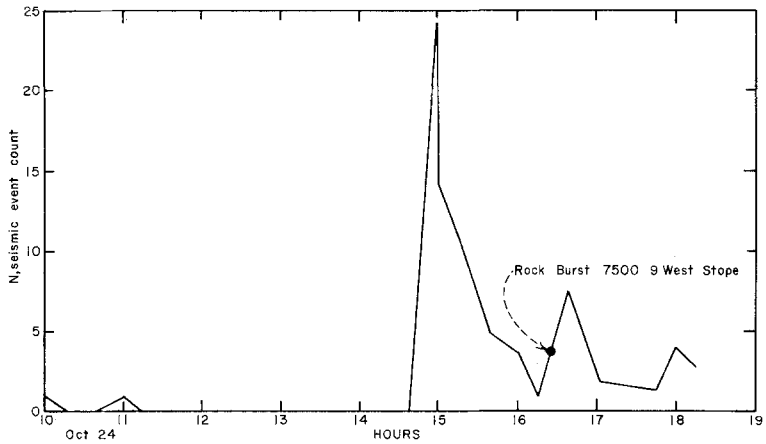

Figure 4
Seismic count (N) against time (hours) for 24 October, 1975, rock burst.

The seismicity increase occurred in a highly localized region shown in Fig. 5. The time duration, τ_d, of this increase was equal to 434 seconds, and mapped out an elliptical zone of area, A_i, equal to approximately 1.78×10^6 cm^2. The aftershock area, A, is equal to approximately 3.55×10^7 cm^2. Thus, the observed ratio τ_0/τ_{do} is equal to approximately 20.0, in close agreement with the value (21.8) obtained from the 3 September burst, the estimated time to this burst, τ_0, is 21.8 τ_0, or 9460 sec (=158 minutes). This value compares with the observed time, τ, of approximately 5239 sec (=87 minutes), a factor of two lower than the predicted value of 158 minutes.

Analysis of the seismic data for this burst reveals two interesting observations. *First*, while the seismicity behavior following the formation of the primary inclusion zone of this burst closely paralleled the behavior observed for the 3 September burst, there was a large seismic event (see solid arrow, Fig. 5) near the hypocenter of the burst that occurred approximately 6 minutes prior to the burst. This event was of sufficient strength to be recorded on the seismograph located on the surface of the mine and may possibly have led to a premature triggering of the mainshock. This behavior is similar to large foreshocks in the hypocentral regions of some large earthquakes just prior (~few hours) to the mainshock. *Second*, the aftershock data suggest a general lack of concentration. This observation can be interpreted in terms of the inclusion theory as indicating that the focal region of this burst may have had

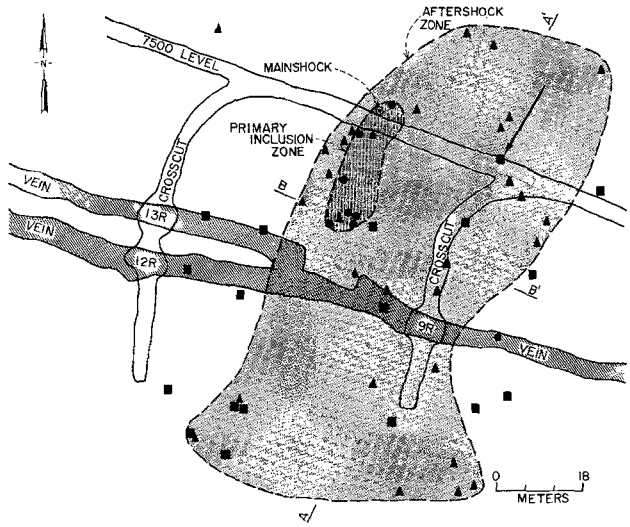

Figure 5
Plan view of 7500 level of the Star mine including aftershock region 'primary inclusion zone', and burst epicenter of 24 October 1975, rock burst. Symbols (circles, squares, triangles) have the same meaning as in Fig. 2. Note the location of the arrow. This event occurred approximately 7 minutes prior to the mainshock and radiated sufficient energy to trigger the surface seismograph.

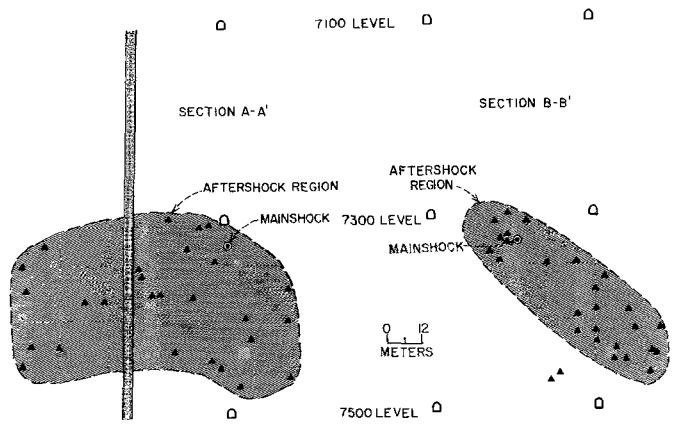

Figure 6
Vertical section of aftershock region of 24 October 1975, rock burst along sections *A–A'* (a) and *B–B'* (b). Symbols (circles, squares, triangles) have the same meaning as in Fig. 2.

enough time required for the storage of strain energy. The reader will recall that precursor time in the inclusion theory denotes the time interval during which the focal region of an impending failure stores strain energy. Similar behavior, that is, possible triggering of failures by large foreshocks, has been observed prior to some major shallow earthquakes [3].

The reader may, at this time, be somewhat puzzled by the observation that the numbers of foreshocks and aftershocks for both the 3 September and 24 October bursts appear to be comparable in number. It is quite likely, however, that the numbers of aftershocks are greater than reported here as the computer is saturated during the first several minutes or so following the burst. This type of behavior is also observed with bursts that occur in the Galena mine.

The 8 October 1975 rock burst sequence

A sequence of rock bursts, who strengths were considerably less than the 3 September and 24 October events, but nevertheless large enough to be registered on the seismograph located on the surface of the Star mine, occurred on the 7500 level of the Star mine on 8 October 1975. Figure 7 illustrates the seismic event count

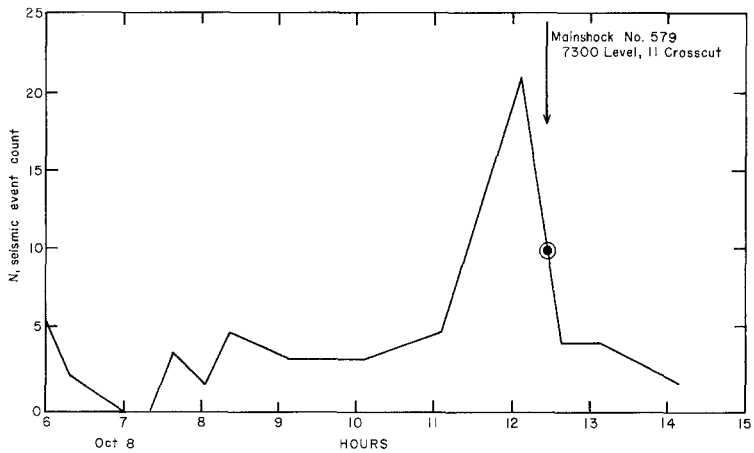

Figure 7
Seismic count (N) against time (hours) for 8 October 1975, rock burst sequence.

against time during 8 October. *Men were prohibited from entering 7500–9 west stope on the basis of this apparent seismicity increase.* A small, damaging rock burst occurred at 12:53:32 (#579, Table 3) shortly after the men were prohibited from entering the stope.

There are features of this burst that are readily distinguishable from the 3 September and 24 October bursts, and as such, demonstrate that a seismicity increase followed by a decrease is not a necessary and sufficient condition for failure to occur, although in this situation, a small burst actually occurred. For example, the seismicity behavior is distinctly different, as is apparent from examination of Figs. 1, 4, and 7. In addition, while increases in Fig. 1 and 4 are both interpreted as being associated with the formation of primary inclusion zones that led to the bursts, the seismicity increase

Table 3

Data relating to 8 October 1975, rockburst sequence

Burst number	Time	Aftershock area (A) (cm^2)	Precursor time (τ_0) calculated (min)	Primary inclusion formation time (τ_{do}) calculated (min)
522	6:08:09	7.86×10^6	31	1.6
562	11:41:56	3.75×10^6	15.2	0.8
569	12:40:08	5.77×10^6	23	1.2
579*	12:53:32	3.47×10^6	14	0.7
589	13:16:38	8.47×10^5	3.4	0.2

* Damaging burst (note inferred rupture direction toward mine workings).

associated with the 8 October burst was apparently due to aftershocks from events 562 and 569, and not to the formation of a primary inclusion zone (Fig. 8). The apparent decrease was associated with the 'normal' hyperbolic aftershock behavior of events 562 and 569.

In the 8 October burst sequence, *no* seismic events were detected in the hypocentral regions prior to the occurrence of the damaging burst (event 579). The low intensities of events 522, 562, 569, 579, and 589, listed in Table 3, are inferred both by observation of mine damage and their recording on the surface seismograph. In addition, the

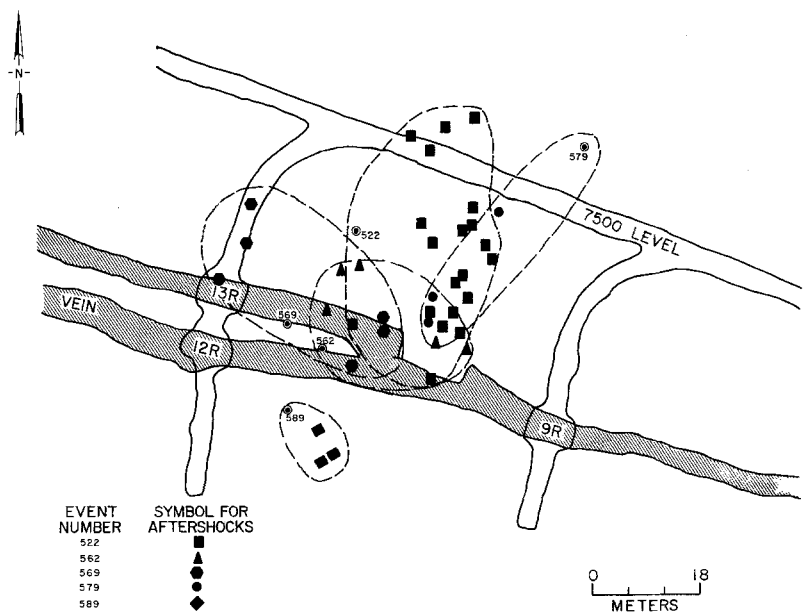

Figure 8

Plan view of 7500 level of the Star mine illustrating aftershock regions of the four low strength seismic events that occurred 8 October 1975.

low strengths of these same events suggest that the (inferred) seismic events that may have produced the primary inclusion zones of events listed in Table 3 may not have had sufficient energy to trigger the required five geophones so as to be recorded on the mine computer. Note also that the calculated formation times (τ_0) listed in Table 3 for these bursts are small ($\sim$several minutes), which adds support to this conjecture. Each of these bursts, listed in Table 3, was recorded on the seismograph located on the surface of the mine. The relative amplitudes of their seismic signatures were found to correspond with the observed aftershock areas of each burst, that is, the larger the aftershock area, the larger the peak-to-peak displacement recorded on the seismograph for the event. Event 579 was observed to have the largest peak-to-peak displacement.

Lastly, it is of interest to note that event 569 may have been instrumental in triggering the damaging burst 579. The calculated time, τ_0, for 579 would have been 14.1 minutes. The observed time interval between 569 and 579 was 13.5 minutes.

Discussion

Based upon the three cases of anomalous seismicity behavior discussed in this article, miners were either evacuated (3 September and 24 October) or prohibited (8 October) from entering regions where moderate rock bursts occurred. Interpretation of the seismicity that preceded each burst shows that the increased seismicity of the 3 September and 24 October bursts was associated with the development of zones of apparent concentrated dilatancy, termed primary inclusion zones, in the hypocentral region of the impending bursts. The seismicity increase and its associated decrease prior to the damaging but small 8 October burst were due to aftershocks of the preceding small bursts, and not the formation of a primary inclusion zone (PIZ) as was the case in the 3 September and 24 October bursts. Data to correctly analyze the 8 October damaging burst (#579, Table 3) were not available because of its apparent very low magnitude, although there is no way to test this conjecture. The 8 October burst sequence (Table 3) does, however, point out the difficulties in predicting small bursts in mines, as such bursts can inflict severe damage to miners who may be located in the immediate vicinity of these bursts.

Experimental data presented in this article and elsewhere [1–5] support the hypothesis that failure of rock materials satisfies a scale-invariant process. Because of this property, these data indicate that reliable prediction of impending failure is a distinct possibility. The time intervals over which the anomalies develop on the intermediate scale are on the order of a few minutes or hours. Thus, prediction of failures on the intermediate scale, such as mine failures like rock bursts, coal bumps, gas outbursts, roof failures, and slope failures, should be possible.

A word of caution on using seismicity anomalies as predictors of impending failure is in order. In the inclusion theory, the seismicity anomaly, that is, seismicity

increase followed by a decrease, which is associated with the formation of a primary inclusion zone, is both a necessary and sufficient condition for the occurrence of failure. However, the converse is not true. A seismicity increase followed by a decrease is not a sufficient condition for an impending failure. Seismicity behavior, in order to be utilized as a predictor of failure, must satisfy certain requirements. First, the siesmicity must be associated with the formation of a primary inclusion zone (PIZ). Once this zone has formed, the system *must* evolve to failure. Second, the seismic events that form the PIZ must be characterized by anomalously long rupture lengths because these seismic events are forming within a stress field whose least principal stress is either zero or tensile [3]. Thus, these events are predicted to exhibit spectra shifted toward low frequencies in comparison with the events that occur in the surrounding medium. Consequently, the energy that would normally be dissipated in frictional processes is now available to power crack growth. This type of analysis is required to determine absolutely that a PIZ of an impending burst has formed. This aspect of the prediction problem is now under active investigation in the Coeur d'Alene mining district.

Implications for earthquake prediction

Figure 9 illustrates the predicted precursor time, τ_0, in seconds against 'effective length', L, in centimeters of selected failures, including a rock burst in the Galena mine [located in the same mining district as the Star mine] [2], a coal mine roof fall in Pennsylvania [2], laboratory size rock failures [4], and several earthquakes. Precursor time, τ_0, refers to the time interval between the initiation of the process that leads to the occurrence of the failure and the actual occurrence of the rupture. This process, once begun, proceeds independently of any changes in the far-field boundary conditions and any changes in material properties within the PIZ and its associated focal region, such as might occur by creep related processes [3]. These changes can, however, produce changes in the time required for storage of strain energy in the focal region of the PIZ. The 'effective length' denotes an *average* linear dimension of the aftershock region that is generated by the failure. The 3 September and 24 October Star events are also shown in Fig. 9. The average 'effective lengths' for these events were calculated by approximating the observed elliptical shaped aftershock areas as circular zones of average diameters of 45 meters and 55 meters, respectively.

Two important observations can be drawn from the data listed in Fig. 9. First, failure of a wide variety of rock materials satisfies a scale invariant process. By scale invariance is meant that the physical processes that lead to failure are independent of scale. Thus, an understanding of the physical processes which lead to failure on the small (laboratory) scale admits an understanding of physical processes leading to failure on the intermediate (mine) scale and the large scale, such as earthquakes. Second, since the relationship between τ_0 and A is approximately linear, and since observational data suggest that earthquakes occur repeatedly in the same region,

apparently on preexisting fault planes, it does not appear to be important to the physical processes which lead irrevocably to failure whether failure occurs in fresh, unbroken material (such as laboratory failures and rock bursts listed in Fig. 9) or along preexisting fault zones, as clearly most of the earthquakes in Fig. 9 have occurred. This result probably suggests that 'old' fault zones probably heal with time, due perhaps, to high temperatures and deposition of minerals by solutions along the fault zone, prior to the occurrence of the next shock.

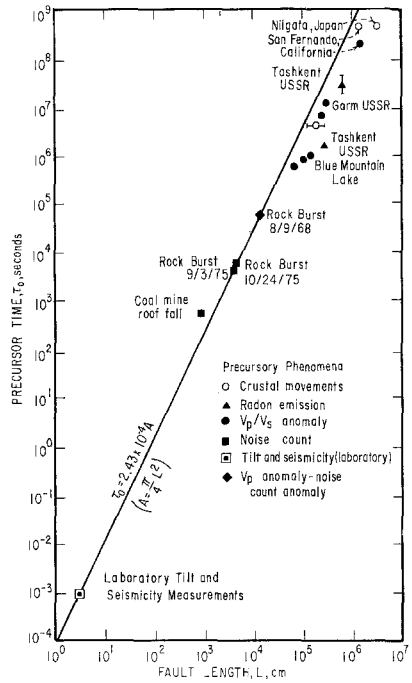

Figure 9
Precursor time – 'fault' length relationships for selected earthquakes, mine failures, and laboratory failures.

Other, perhaps less important, aspects of the data listed in Fig. 9 warrant attention: (1) The relationship between τ_0 and A, shown in Fig. 9, is only valid when changes are not occurring in the far-field boundary conditions during the time interval τ_0. Obviously, this condition can be relaxed, as evidenced by the presence of large foreshocks, such as occur prior to large earthquakes and rock bursts (for example, the 24 October, 1975, Star burst). Foreshocks tend to increase load within the potential failure zone, and consequently, can serve to 'prematurely' trigger the impending failure. (2) Changes (increases) in the far-field boundary strains due to plate motions can shorten the theoretically determined precursor time. These changes are consistent with the inclusion theory as the precursor time is inversely proportional to loading rate changes that occur during the preparation time of the impending

shock. Thus, there is *no* compelling reason to presume that the functional relationship specified by equation 1 (Fig. 9) will hold for all classes of failures. In addition, the reader will note the tendency for precursor times to drop off at increasing sizes of impending failure, probably the result of changes in the far-field stresses due to plate motions occurring during the required preparation time of the impending shock. Note also that the predicted and observed precursor time of approximately 1 ms prior to failure of rock on the laboratory scale should be considered as representing an upper limiting value. For example, shock loading tests, entailing large increases occurring over a short time interval in a material within which a PIZ is nucleated, can decrease the predicted precursor time (τ_0) by several orders of magnitude, the exact value depending on how rapidly the far-field strains are changing.

The ratio τ_0/τ_{do} ($=A/A_i$) was shown earlier to be approximately 21.0 for rock bursts that were known to develop in a rock mass characterized by very low intrinsic porosity. (Intrinsic porosity, ϕ_i, in the context used here, refers to the porosity existing within material prior to the application of applied loads.) Excluded from the magnitude of ϕ_i is any rehealing, due for example, to pressure solution or cementation from pore fluids during the time interval between when the load is applied and the occurrence of failure.

It is shown in the Appendix that the influence of intrinsic porosity on the predicted τ_0 versus A relationship is an important factor in calculating realistic accurate prediction times to failure. The function relationship of τ_0/τ_{do} to ϕ_i is shown to be

$$\tau_0 \simeq \tau_{do} + \tau_{do} \frac{K(\tau_0)}{n} \left(\frac{1 - \phi_0}{1 - \phi} \right), \tag{2}$$

where $\phi_0 = \phi_i + \phi_f + \phi_p$

$\phi = \phi_i$

$n = C_0/T_0$

and ϕ_i = intrinsic porosity of the material,

ϕ_f = fracture porosity prior to the formation of the PIZ,

ϕ_p = fracture porosity within the PIZ due to the seismic events that occurred to form the PIZ,

C_0/T_0 = ratio of uniaxial compressive strength to the tensile strength of the material.

In equation (2), $K(\tau_0)$ is the stress concentration factor existing at the boundary of the PIZ and its associated focal region at the instant of failure.

Two useful results are a direct consequence of equation (2). First, the inclusion theory provides a simple explanation of the transition in material behavior from violent brittle failure occurring in fresh, unbroken materials with no intrinsic porosity ($\phi_i = 0$) to 'quiet' aseismic creep observed to occur along well-fractured fault zones whose intrinsic porosities are high and equal to $\phi_i \simeq 1 - (\phi_f + \phi_p)$. Note that in the latter case, $A \simeq A_i$, that is, the effective tensile strength of the fault zone (gouge) is

approximately zero. Second, the ratio (α) of focal region area (A) to the primary inclusion zone area (A_i), A/A_i, is not an invariant. Its value can range from high ($\simeq 21.8$) for fresh failures in tight, low porosity rock to low ($\simeq 1.0$) along highly fractured fault zones exhibiting aseismic or steady-state creep. A determination of α in given earthquake zones is critical in order to permit accurate predictions of impending earthquakes.

In conclusion, one of the more important findings of this study is that failures on the intermediate (mine) scale and small (laboratory) scale exhibit characteristics consistent with failures on the large scale, such as earthquakes. Thus, failure characteristics of rock bursts, such as their associated foreshocks and aftershocks, should produce results compatible with known observational characteristics of earthquakes. The study of rock bursts, to date, supports this hypothesis, although much more thorough and detailed investigations are required. The Bureau of Mines experience in rock burst prediction, as well as that of the Hecla Mining Company, suggests that reliable and accurate prediction of rock bursts will be difficult. For instance, small bursts (like the 8 October 1975 sequence reported earlier) that have occurred in the Star mine apparently exhibit no seismic anomalies. However, the energy content of these bursts is probably low so as not to register on the existing seismic network. Similarly, large bursts ($M_L \geq 2.0$), which are often located several tens to hundreds of meters from the mine workings, have occurred with no observable seismicity anomaly. This class of bursts has been observed in both the Star and Galena mines, both of which have active seismic networks. Our preliminary studies suggest these bursts occur along old fault zones that are apparently activated by the mining process. A working hypothesis at this time is that these bursts occur along existing zones that are 'hung up' along small asperities or lock points. Failure of the asperities, showing perhaps the classic seismic anomaly discussed earlier but too small to register on the existing network, causes releases of strain energy that had been stored along the fault zone by nearby mining operations. *Thus, if the characteristics of rock bursts carry over to large-scale failure phenomena, and preliminary data suggest this to be the case,* then it is conceivable that a low-magnitude earthquake, predicted to occur along an active fault zone, could release stored strain energy outside the locked zone and produce an energy release equivalent to a *much larger* shock. This situation clearly requires further study.

Acknowledgments

The Hecla Mining Co., Wallace, Idaho, generously provided the data used in this report. In particular, special thanks are due to Jon Langstaff, Senior Rock Mechanics Engineer, Hecla Mining Co., for discussions of this data. The opinions expressed in this report represent those of the author and not necessarily those of the Hecla Mining Co. W. Spence, R. Martin, and in particular, M. Wyss offered valuable comments on early drafts of this manuscript.

APPENDIX

Effect of intrinsic porosity on the precursor time-aftershock area relationship

Intrinsic porosity, ϕ_i, will be defined as the porosity existing within a material prior to the application of applied loads. Excluded from the value of ϕ_i is any re-healing due, for example, to pressure solution or cementation resulting from pore fluids, that may occur during the time interval between load application and the occurrence of failure.

Let σ_t and σ_c denote the local values of the tensile and compressive stresses, in a direction normal to the eventual rupture propagation direction, existing within the evolving PIZ and its associated focal region at a time, t, prior to the mainshock. Force equilibrium in the material requires

$$\int \sigma_t \, dA_i = \int \sigma_c \, dA, \quad 0 \leq t \leq \tau_0 \tag{A1}$$

where the integration is over the *solid* cross sectional areas. It is assumed, for calculational simplicity, that no changes occur in the far-field boundary conditions during the preparation time required for the failure. For ease of calculation, assume the stresses in equation A1 are uniform throughout their respective areas of integration. Thus, to a first-order approximation

$$\bar{\sigma}_t A_i^* \simeq \bar{\sigma}_c A^*,$$

where

$$\bar{\sigma}_t = \frac{1}{A_i^*} \int \sigma_t \, dA_i \quad , \quad \bar{\sigma}_c = \frac{1}{A_i^*} \int \sigma_c \, dA \tag{A3}$$

and A_i^* and A^* represent the effective solid cross sectional areas of the PIZ and its associated focal region. Define

ϕ_i = intrinsic porosity of the material,
ϕ_f = fracture porosity existing in the material prior to the formation of the PIZ,
ϕ_p = fracture porosity induced within the PIZ during the formation of the PIZ.

Equations 1, A1, and A2 can then be combined to give the total time required for the failure preparation process $\{[A_i^* = A_i(1 - \phi_0), A^* = A(1 - \phi(t)]\}$

$$\tau \simeq \tau_{do} + \frac{\bar{\sigma}_c \tau_{do}}{\bar{\sigma}_t \phi_p} \frac{1 - \phi_0}{1 - \phi(t)}, \tag{A4}$$

where $\phi_0 = \phi_i + \phi_f + \phi_p$, $\phi = \phi_f(t)$, and $\tau/\tau_{do} = A/A_i$. Note that the fracture porosity, ϕ_f, existing within the focal region of the evolving PIZ is time dependent, since cracks within this region will close in response to an increasing level in $\bar{\sigma}_c$ as the system evolves to failure.

In the inclusion theory, a long, narrow macrocrack forms within the primary

inclusion zone at the instant of failure. Let the value of $\bar{\sigma}_t$ just prior to crack coalescence be denoted by T_0, where T_0 denotes the uniaxial tensile strength of the material. Let $C_0 = K(\tau_0)\bar{\sigma}_c$, where C_0 is the uniaxial compressive strength of the material at the boundary between the PIZ and its focal region, and $K(\tau_0)$ is a stress concentration factor denoting the ratio of C_0 to the average compressive stress existing in the focal region of the impending failure at the instant of failure. Equation A4 becomes

$$\tau_0 \simeq \tau_{do} + \tau_{do} \frac{K(\tau_0)}{n\phi_p} \frac{1 - \phi_0}{1 - \phi_i},$$

where $\phi(t)$, at time $t = \tau_0$, is assumed to ϕ_i, i.e., $\phi_i(\tau_0) \simeq 0$ throughout the focal region, and $n = C_0/T_0$. The relationship between A and A_i can then be written

$$\alpha = \frac{A}{A_i} \simeq 1 + \frac{K(\tau_0)}{n\phi_p} \frac{1 - \phi_0}{1 - \phi_i}. \tag{A6}$$

Equations A5 and A6 show that both precursor time, τ_0, and aftershock area, A, decrease as the intrinsic porosity, ϕ_i, of the material increases. For example, τ_0 and A attain their maximum possible values when $\phi_i = 0$ and their lowest values, τ_{do} and A_i, respectively, in the limit as ϕ_i approaches $1 - (\phi_f + \phi_p)$. The effective tensile strength of the material is identically zero under these conditions. No seismicity anomaly will be observed on any scale of failure, in the unlikely situation that ϕ_i remains scale invariant. The system enters a state of aseismic or steady-state creep at this time.

The rock burst data reported in the test provide a reasonable upper limit for α ($\simeq 21$) in equation A6. In this situation

$$K(\tau_0) \simeq \left[\frac{20n}{1 - (\phi_f + \phi_p)}\right]^{-1} \tag{A7}$$

The theoretical ratio of the compressive strength, that is, the value of the applied compressive stress required to initiate crack growth from a critically oriented flaw, to the tensile strength, n, is provided by the Griffith model of failure. The result is $n = 8.0$. Thus, $K(\tau_0 \simeq 0.006[1 - (\phi_f + \phi_p)]$, or simply, the stress concentration factor at the PIZ–focal region boundary is dependent only on the total fracture porosity existing within the PIZ at a time just prior to crack coalescence in this zone. A reasonable value for $(\phi_f + \phi_p)$ is 0.5, giving $K(\tau_0) \simeq 0.003$. To a first-order approximation, the quantities $K(\tau_0)$, n, and $(\phi_f + \phi_p)$ are scale invariant.

References

[1] Aggarwal, Y. P., Sykes, L. R., Armbruster, J. and Sbar, M. L. (1973), *Premonitory changes in seismic velocities and prediction of earthquakes*, Nature *241*, 5385.

[2] Brady, B. T. (1974), *Seismic precursors before rock failures in mines*, Nature *252*, 5484.

[3] BRADY, B. T. (1966), *Theory of earthquakes, IV. General implications for earthquake prediction*, Pure appl. Geophys. (in press).

[4] BRADY, B. T. (1977), *An investigation of the scale invariant properties of failure*, Int. J. Rock Mech. Mining Sci. (in press).

[5] NERSESOV, I. L., LUKK, A. A., PONOMAREV, V. S., RAUTAIN, T. G., RULEV, B. G., SEMENOV, A. N. and SIMBRIEVA, I. G., *Possibilities of Earthquake Prediction Exemplified by the Garm Area of the Tadzhik, S.S.R., in Earthquake Precursors* (ed. M. A. Sadovskii, I. L. Nersesov and L. G. Latynina) (U.S.S.R. Academy of Sciences, Moscow 1975), pp. 79–99.

[6] MCWILLIAMS, J. R. and ERICKSON, E. G., *Methods and Costs of Shaft Sinking in the Coeur d'Alene District, Shoshone County, Idaho*, (BuMines IC 7961, 1960).

[7] LANGSTAFF, J., *Hecla's seismic detection system*, Proceedings of the 17th Rock Mechanics Symposium, Snowbird, Utah, 1976.

(Received 2nd November 1976)